IJARCCE ISSN (O) 2278-1021, ISSN (P) 2319-5940

International Journal of Advanced Research in Computer and Communication Engineering

Impact Factor 8.471 ⁙ Peer-reviewed & Refereed journal ⁙ Vol. 15, Issue 8, August 2026

DOI: 10.17148/IJARCCE.2026.15838

A Robust Multi-Stage Framework for Noise-Resilient Bone Tumor Detection, Segmentation, and Classification

V.Dineshkumar[1], Dr. N. Kamaraj[2]

Research Scholar & Assistant Professor, Department of Computer Science,

Sri Ramakrishna Mission Vidyalaya College of Arts and Science, Coimbatore, India[1]

Head & Assistant Professor, Department of Information Technology,

Sri Ramakrishna Mission Vidyalaya College of Arts and Science, Coimbatore, India[2]

Abstract: Accurate identification and segmentation of bone tumors from medical images are essential for early diagnosis, treatment planning, and prognosis estimation. However, automated analysis remains difficult because bone lesions show considerable variation in shape, size, texture, anatomical location, and boundary definition, while medical images are frequently affected by noise and low contrast. This research work presents a three-phase framework for bone tumor analysis. In Phase 1, image normalization, noise reduction, contrast enhancement, adaptive superpixels, and stochastic clustering based on Gaussian Mixture Models and Expectation-Maximization are used for noise-resilient candidate-region segmentation. In Phase 2, a Fast Mask R-CNN architecture with a VGG-19 backbone is employed for simultaneous tumor localization, segmentation, and benign/malignant classification. In Phase 3, Snake Swarm Optimization (SSO) is integrated to refine segmentation boundaries and optimize key model parameters. This results show progressive improvement across phases: the Phase 1 model achieved 96.3% accuracy, 90.5% sensitivity, 97.89% Dice coefficient, and 96.86% Jaccard index; the Phase 2 model achieved 96.31% accuracy, 94.25% precision, 97.82% recall, and 95.99% F1-score; and the optimized Phase 3 model achieved 97.8% accuracy, 97.2% precision, 97.9% recall, and 97.5% F1-score. Collectively, the findings suggest that combining adaptive segmentation, instance segmentation, and swarm-based optimization can improve robustness and clinical usefulness in computer-aided bone tumor diagnosis.

Keywords: bone tumor; medical image segmentation; Fast Mask R-CNN; adaptive superpixels; Gaussian mixture model; expectation-maximization; Snake Swarm Optimization; computer-aided diagnosis.

I. INTRODUCTION

Bone tumors are abnormal proliferative lesions of osseous tissue that may be benign, malignant, or metastatic. Clinical management depends heavily on accurate lesion localization, extent estimation, and characterization because malignant tumors such as osteosarcoma often require aggressive intervention, while benign lesions may need only observation or limited surgery [1-4]. Radiographs, computed tomography (CT), and magnetic resonance imaging (MRI) remain central to diagnosis; however, manual interpretation is time consuming and subject to inter-observer variability [1-5].

In recent years, machine learning and deep learning have significantly improved the automated analysis of medical images [11,12,21,22]. For bone tumor imaging, the major unresolved issues are image noise, heterogeneous tumor appearance, complex boundaries, and the difficulty of unifying detection, segmentation, and classification in a single framework [2-9]. The research directly addresses these challenges through a staged methodology that evolves from stochastic segmentation to deep instance segmentation and finally to optimization-assisted refinement.

The main contributions are as follows: (i) a noise-resilient preprocessing and adaptive-superpixel segmentation stage; (ii) a multi-class Fast Mask R-CNN framework for lesion localization, segmentation, and classification; and (iii) an enhanced optimization stage using Snake Swarm Optimization to improve tumor boundary delineation and classification robustness [14-16,23,24,27-30].

II. RELATED WORK

A. Conventional and stochastic segmentation

Before the rise of deep learning, bone and tumor segmentation commonly relied on thresholding, region growing, active contours, watershed methods, superpixel partitioning, and clustering-based schemes. Such methods are useful because they are interpretable and computationally economical; nevertheless, they often degrade in the presence of noise, intensity

© IJARCCE This work is licensed under a Creative Commons Attribution 4.0 International License

DOI: 10.17148/IJARCCE.2026.15838

inhomogeneity, and irregular lesion morphology [4,8,23,24]. Adaptive superpixels generated with SLIC preserve local image structure and can reduce computational burden by grouping perceptually similar pixels [23]. Expectation-Maximization (EM) with Gaussian Mixture Models (GMMs) further supports probabilistic clustering and can handle uncertainty in tissue assignment [24].

B. Deep learning for bone tumor analysis

Deep convolutional neural networks have transformed medical image analysis by learning hierarchical representations from raw image data [11]. U-Net and FCN architectures established the basis for modern biomedical image segmentation by combining localization and semantic feature learning [12,13], while V-Net and nnU-Net extended this paradigm to volumetric and self-configuring segmentation settings [21,22]. For bone tumors, Potter et al. used CT data for segmentation and classification [1], von Schacky et al. proposed multitask learning on radiographs [2], and Ye et al. reported multi-task ensemble learning on MRI data [3]. Additional studies have explored Seg-Unet, hybrid CNN–ViT designs, and bone scan segmentation methods [5-8].

C. Detection, classification, and optimization frameworks

Instance segmentation models are especially relevant to bone tumor analysis because they can jointly identify a lesion, localize it spatially, and produce a pixel-wise mask. Faster R-CNN introduced region proposal networks for efficient object detection [15], and Mask R-CNN subsequently added a parallel mask branch for instance segmentation [14]. VGG [16], ResNet [17], DenseNet [18], YOLO [19], and Vision Transformers (ViT) [20] have been used as backbones or comparative baselines in medical imaging. Optimization strategies can further refine learned models. In particular, Snake Optimizer is a recent population-based metaheuristic with strong exploration–exploitation behavior [27]. The three related studies progressively applied these concepts to bone tumor analysis [28–30].

III. MATERIALS AND METHODS

A. Study design and data source

The proposed framework follows a three-phase design. This research data were obtained from a publicly available Kaggle bone tumor resource and consist of annotated bone tumor medical images suitable for segmentation and classification. Across the three phases, preprocessing includes normalization, denoising, and contrast enhancement to improve the visibility of lesion regions and reduce variability caused by acquisition conditions. These steps are intended to provide a consistent input representation for both stochastic and deep learning stages.

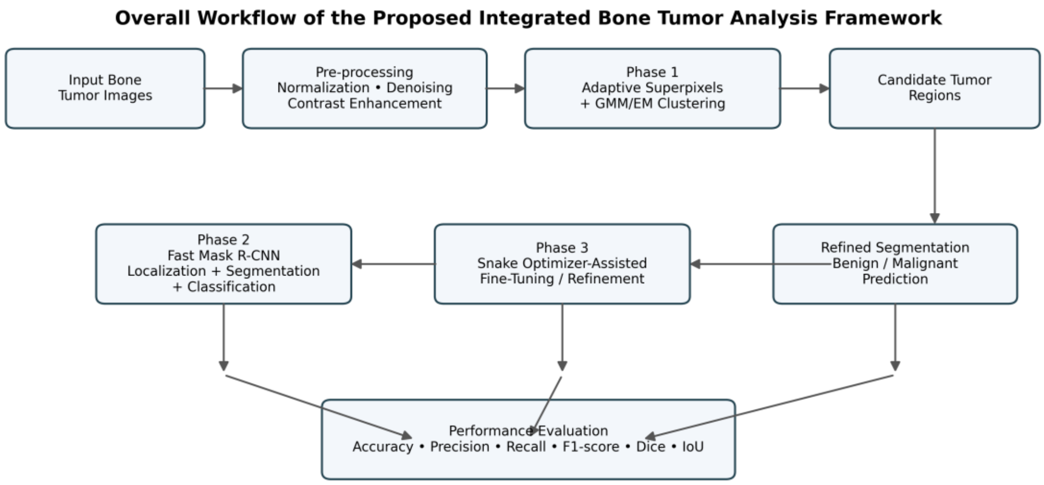

Fig. 1 Overall workflow of the proposed integrated bone tumor analysis framework

B. Phase 1: adaptive superpixels and stochastic clustering

Phase 1 focuses on noise-resilient tumor identification. After preprocessing, the image is partitioned into adaptive superpixels so that local structural information is preserved while reducing pixel-level complexity [23]. Candidate tumor regions are then segmented using a stochastic clustering strategy built on GMM and EM [24]. The cluster outputs are combined in an ensemble manner, followed by adaptive thresholding and post-processing to suppress artifacts and obtain realistic lesion shapes. According to the research work, this phase is particularly beneficial when lesion appearance is highly heterogeneous or when radiographic noise complicates boundary extraction [28].

 This work is licensed under a Creative Commons Attribution 4.0 International License

IJARCCE ISSN (O) 2278-1021, ISSN (P) 2319-5940

International Journal of Advanced Research in Computer and Communication Engineering

Impact Factor 8.471 ⁜ Peer-reviewed & Refereed journal ⁜ Vol. 15, Issue 8, August 2026

DOI: 10.17148/IJARCCE.2026.15838

A simplified formulation of the adaptive clustering stage can be summarized as follows:
• Accuracy = (TP + TN) / (TP + TN + FP + FN)
• Precision = TP / (TP + FP)
• Recall = TP / (TP + FN)
• Ensemble probability: P_ensemble(x) = (1/N) Σ P_i(x)

C. Phase 2: Fast Mask R-CNN for segmentation and classification

Phase 2 extends the framework to simultaneous lesion localization, segmentation, and classification using Fast Mask R-CNN. The model employs a VGG-19 backbone for feature extraction [16], region proposal generation inspired by Faster R-CNN [15], RoI alignment, and parallel branches for class prediction and mask estimation [14]. Transfer learning is used to initialize convolutional features, after which the model is fine-tuned on the bone tumor images. The phase is designed to distinguish at least benign and malignant classes while producing spatially precise masks [2,14,29].

D. Phase 3: Snake Swarm Optimization-assisted refinement

In Phase 3, the instance segmentation framework is enhanced by a metaheuristic optimization stage. Snake Swarm Optimization (SSO) is used to refine model parameters and improve lesion boundary delineation [27]. The reserach states that the optimizer is applied to parameters such as anchor sizes, learning rates, and mask thresholds, while boundary refinement is guided by snake-like control-point evolution. This optimization-assisted strategy is intended to reduce false positives, improve boundary adherence, and strengthen classification performance in difficult cases [30].

E. Evaluation metrics

Classification performance is evaluated using accuracy, precision, recall, and F1-score. Segmentation performance is assessed using overlap measures such as Dice coefficient and Intersection over Union (IoU/Jaccard index) [25,26]. The main formulas used in the manuscript are listed below:

• F1-score = 2 × (Precision × Recall) / (Precision + Recall)

• Dice coefficient = 2|X ∩ Y| / (|X| + |Y|)

• IoU (Jaccard index) = |X ∩ Y| / |X ∪ Y|

IV. RESULTS AND DISCUSSION

The research reports progressive improvement from Phase 1 to Phase 3. Because the supplied research work fully clarifies the all models were evaluated on identical splits and protocols, the values should be interpreted as reported phase-wise outcomes rather than as a fully controlled head-to-head experiment. Nevertheless, the pattern consistently shows that the integrated framework improves robustness and predictive performance across successive stages.

TABLE 1. PHASE-WISE PERFORMANCE VALUES REPORTED IN THE RESEARCH

Method	Accuracy (%)	Precision (%)	Recall/Sensitivity (%)	F1-score (%)	Dice (%)	IoU/Jaccard (%)
Phase 1: Adaptive superpixels + GMM/EM	96.30	—	90.50	—	97.89	96.86
Phase 2: Fast Mask R-CNN	96.31	94.25	97.82	95.99	—	—
Phase 3: Fast Mask R-CNN + SSO	97.80	97.20	97.90	97.50	—	—

International Journal of Advanced Research in Computer and Communication Engineering
Impact Factor 8.471 ⁑ Peer-reviewed & Refereed journal ⁑ Vol. 15, Issue 8, August 2026
DOI: 10.17148/IJARCCE.2026.15838

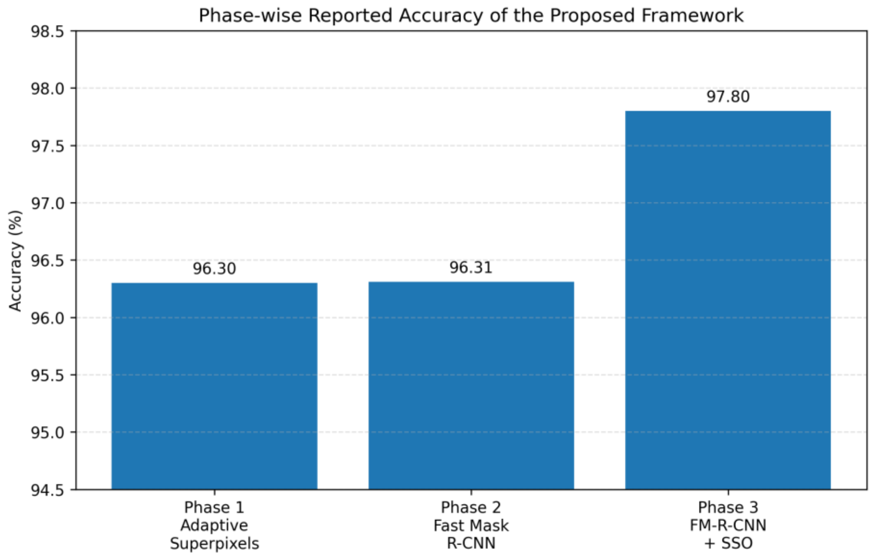

Fig. 1 Phase-wise reported accuracy of the proposed framework based on work-reported results

In Phase 1, the proposed stochastic framework outperformed conventional baselines such as active contours, biorthogonal wavelets, seeded region growing, and Canny-based segmentation as reported in the work. The high Dice coefficient (97.89%) and Jaccard index (96.86%) indicate strong overlap between predicted and reference tumor regions. Phase 2 retained high accuracy (96.31%) while extending the framework to simultaneous classification and segmentation. The strongest performance was observed in Phase 3, where optimization-assisted refinement yielded 97.8% accuracy, 97.2% precision, 97.9% recall, and 97.5% F1-score, suggesting that SSO improves both sensitivity and prediction stability.

From a methodological perspective, the three phases are complementary rather than redundant. Phase 1 enhances noise resilience and preserves local structure; Phase 2 provides end-to-end lesion localization and classification; and Phase 3 improves parameter tuning and contour refinement. This integration is relevant to orthopedic computer-aided diagnosis because clinical imaging datasets are often heterogeneous and small, making robust preprocessing and careful optimization especially important [4,9,11].

Despite these strengths, several limitations should be acknowledged. First, the journal version should clearly state the exact dataset size, modality distribution, annotation procedure, and patient-level split strategy. Second, external validation on an independent cohort would substantially strengthen claims of generalizability. Third, ablation experiments quantifying the individual contributions of superpixels, Fast Mask R-CNN, and SSO would improve scientific rigor. These additions are recommended for the final submission version.

V. CONCLUSION

The work proposes an integrated three-phase framework that combines adaptive superpixel-based stochastic segmentation, Fast Mask R-CNN instance segmentation, and Snake Swarm Optimization-assisted refinement. The reported results indicate that the framework can deliver high segmentation fidelity and strong classification performance, with the best phase achieving 97.8% accuracy and 97.5% F1-score. Overall, the study demonstrates the potential of combining classical image processing, deep learning, and metaheuristic optimization to support clinically useful computer-aided diagnosis of bone tumors. Future work should prioritize external validation, multimodal imaging, and prospective clinical evaluation.

REFERENCES

[1]. Yildiz Potter I, Yeritsyan D, Mahar S, Wu J, Nazarian A, Vaziri A, Vaziri A. Automated bone tumor segmentation and classification as benign or malignant using computed tomographic imaging. Journal of Digital Imaging. 2023;36(3):869-878. doi:10.1007/s10278-022-00771-z.

[2]. Von Schacky CE, Wilhelm NJ, Schäfer VS, Leonhardt Y, Gassert FG, Foreman SC, et al. Multitask deep learning for segmentation and classification of primary bone tumors on radiographs. Radiology. 2021;301(2):398-406. doi:10.1148/radiol.2021204531.

ISSN (O) 2278-1021, ISSN (P) 2319-5940
International Journal of Advanced Research in Computer and Communication Engineering
Impact Factor 8.471 ⁒ Peer-reviewed & Refereed journal ⁒ Vol. 15, Issue 8, August 2026
DOI: 10.17148/IJARCCE.2026.15838

[3]. Ye Q, Yang H, Lin B, Wang M, Song L, Xie Z, et al. Automatic detection, segmentation, and classification of primary bone tumors and bone infections using an ensemble multi-task deep learning framework on multi-parametric MRIs: a multi-center study. European Radiology. 2024;34(7):4287-4299. doi:10.1007/s00330-023-10506-5.
[4]. Paranavithana IR, Stirling D, Ros M, Field M. Systematic review of tumor segmentation strategies for bone metastases. Cancers. 2023;15(6):1750. doi:10.3390/cancers15061750.
[5]. Chen W, Ayoub M, Liao M, Shi R, Zhang M, Su F, et al. A fusion of VGG-16 and ViT models for improving bone tumor classification in computed tomography. Journal of Bone Oncology. 2023;43:100508. doi:10.1016/j.jbo.2023.100508.
[6]. Do NT, Jung ST, Yang HJ, Kim SH. End-to-end bone tumor segmentation and classification from X-ray images by using multi-level Seg-Unet model. Journal of KIISE. 2020;47(2):170-179. doi:10.5626/JOK.2020.47.2.170.
[7]. Do NT, Jung ST, Yang HJ, Kim SH. Multi-level Seg-Unet model with global and patch-based X-ray images for knee bone tumor detection. Diagnostics. 2021;11(4):691. doi:10.3390/diagnostics11040691.
[8]. Chu G, Lo P, Ramakrishna B, Kim H, Morris D, Goldin J, Brown M. Bone tumor segmentation on bone scans using context information and random forests. In: Medical Image Computing and Computer-Assisted Intervention – MICCAI 2014. Cham: Springer; 2014. p. 601-608. doi:10.1007/978-3-319-10404-1_75.
[9]. Zhou X, Wang H, Feng C, Xu R, He Y, Li L, Tu C. Emerging applications of deep learning in bone tumors: current advances and challenges. Frontiers in Oncology. 2022;12:908873. doi:10.3389/fonc.2022.908873.
[10]. Biratu ES, Schwenker F, Ayano YM, Debelee TG. A survey of brain tumor segmentation and classification algorithms. Journal of Imaging. 2021;7(9):179. doi:10.3390/jimaging7090179.
[11]. Litjens G, Kooi T, Bejnordi BE, Setio AAA, Ciompi F, Ghafoorian M, et al. A survey on deep learning in medical image analysis. Medical Image Analysis. 2017;42:60-88. doi:10.1016/j.media.2017.07.005.
[12]. Ronneberger O, Fischer P, Brox T. U-Net: Convolutional networks for biomedical image segmentation. In: Medical Image Computing and Computer-Assisted Intervention – MICCAI 2015. Cham: Springer; 2015. p. 234-241. doi:10.1007/978-3-319-24574-4_28.
[13]. Long J, Shelhamer E, Darrell T. Fully convolutional networks for semantic segmentation. In: Proceedings of the IEEE Conference on Computer Vision and Pattern Recognition. 2015. p. 3431-3440. doi:10.1109/CVPR.2015.7298965.
[14]. He K, Gkioxari G, Dollár P, Girshick R. Mask R-CNN. In: Proceedings of the IEEE International Conference on Computer Vision. 2017. p. 2961-2969. doi:10.1109/ICCV.2017.322.
[15]. Ren S, He K, Girshick R, Sun J. Faster R-CNN: Towards real-time object detection with region proposal networks. IEEE Transactions on Pattern Analysis and Machine Intelligence. 2017;39(6):1137-1149. doi:10.1109/TPAMI.2016.2577031.
[16]. Simonyan K, Zisserman A. Very deep convolutional networks for large-scale image recognition. International Conference on Learning Representations. 2015. arXiv:1409.1556.
[17]. He K, Zhang X, Ren S, Sun J. Deep residual learning for image recognition. In: Proceedings of the IEEE Conference on Computer Vision and Pattern Recognition. 2016. p. 770-778. doi:10.1109/CVPR.2016.90.
[18]. Huang G, Liu Z, van der Maaten L, Weinberger KQ. Densely connected convolutional networks. In: Proceedings of the IEEE Conference on Computer Vision and Pattern Recognition. 2017. p. 4700-4708. doi:10.1109/CVPR.2017.243.
[19]. Redmon J, Divvala S, Girshick R, Farhadi A. You only look once: Unified, real-time object detection. In: Proceedings of the IEEE Conference on Computer Vision and Pattern Recognition. 2016. p. 779-788. doi:10.1109/CVPR.2016.91.
[20]. Dosovitskiy A, Beyer L, Kolesnikov A, Weissenborn D, Zhai X, Unterthiner T, et al. An image is worth 16x16 words: Transformers for image recognition at scale. International Conference on Learning Representations. 2021.
[21]. Isensee F, Jaeger PF, Kohl SAA, Petersen J, Maier-Hein KH. nnU-Net: A self-configuring method for deep learning-based biomedical image segmentation. Nature Methods. 2021;18(2):203-211. doi:10.1038/s41592-020-01008-z.
[22]. Milletari F, Navab N, Ahmadi SA. V-Net: Fully convolutional neural networks for volumetric medical image segmentation. In: Fourth International Conference on 3D Vision. 2016. p. 565-571. doi:10.1109/3DV.2016.79.

© IJARCCE This work is licensed under a Creative Commons Attribution 4.0 International License

ISSN (O) 2278-1021, ISSN (P) 2319-5940

International Journal of Advanced Research in Computer and Communication Engineering

Impact Factor 8.471 ∺ Peer-reviewed & Refereed journal ∺ Vol. 15, Issue 8, August 2026

DOI: 10.17148/IJARCCE.2026.15838

[23]. Achanta R, Shaji A, Smith K, Lucchi A, Fua P, Süsstrunk S. SLIC superpixels compared to state-of-the-art superpixel methods. IEEE Transactions on Pattern Analysis and Machine Intelligence. 2012;34(11):2274-2282. doi:10.1109/TPAMI.2012.120.

[24]. Dempster AP, Laird NM, Rubin DB. Maximum likelihood from incomplete data via the EM algorithm. Journal of the Royal Statistical Society: Series B. 1977;39(1):1-38. doi:10.1111/j.2517-6161.1977.tb01600.x.

[25]. Taha AA, Hanbury A. Metrics for evaluating 3D medical image segmentation: analysis, selection, and tool. BMC Medical Imaging. 2015;15:29. doi:10.1186/s12880-015-0068-x.

[26]. Zou KH, Warfield SK, Bharatha A, Tempany CMC, Kaus MR, Haker SJ, et al. Statistical validation of image segmentation quality based on a spatial overlap index. Academic Radiology. 2004;11(2):178-189. doi:10.1016/S1076-6332(03)00671-8.

[27]. Hashim FA, Hussien AG. Snake Optimizer: a novel meta-heuristic optimization algorithm. Knowledge-Based Systems. 2022;242:108320. doi:10.1016/j.knosys.2022.108320.

[28]. Dineshkumar V, Vijayakumar V. Adaptive superpixels for noise-resilient bone tumor identification in medical imaging. Nanotechnology Perceptions. 2024;20(S12). doi:10.62441/nano-ntp.v20iS12.72.

[29]. Dineshkumar V, Vijayakumar V. Multi-class bone tumor detection and segmentation using Fast Mask R-CNN for precise localization and classification. African Journal of Biological Sciences. 2024;6(6):7794-7806. doi:10.33472/AFJBS.6.6.2024.7794-7806.

[30]. Dineshkumar V, Vijayakumar V. Enhanced Fast Mask R-CNN with Snake Swarm Optimization for precise bone tumor segmentation and classification. South Eastern European Journal of Public Health. 2025;XXVI(S1):4177-4193. doi:10.70135/seejph.vi.4776.

 This work is licensed under a Creative Commons Attribution 4.0 International License